BJES Basrah Journal for Engineering Sciences

OPEN ACCESS

Effect of Spanwise Semicircular Groove on NACA 0012 Airfoil

Mahdi S. Almusawi [1,2]*, Qais A. Rishack [3], Mohammed A. Al-fahham [4]

[1] *Department of Mechanical Engineering, College of Engineering, University of Basrah, Basrah, Iraq*
[2] *Department of Mechanical Engineering, College of Engineering, University of Kufa, Najaf, Iraq*
[3] *Department of Material Engineering, College of Engineering, University of Basrah, Basrah, Iraq*
[4] *Department of Aeronautical Engineering Technical, Engineering Technical College, University of Al-Furat Al-Awsat Technical Al-Najaf, Najaf, Iraq*
E-mail addresses: mehdis.almosawi@uokufa.edu.iq , qais.rashck@uobasrah.edu.iq , coj.moh@atu.edu.iq

Abstract

The efficiency of an airfoil can be improved by adjusting its surface. CFD software was used to investigate a 2D airfoil with and without a spanwise semicircular groove on the upper surface. NACA0012 airfoils with and without grooves were analyzed using the k-ω turbulence model. The lift and drag coefficients were used to compared. To investigate the effect of groove location on airfoil efficiency, a groove was added in various locations and compared to a smooth airfoil. The flow velocity remained constant at 20 m/s at all angles of attack (AOA). According to this study, which used ANSYS software to simulate it numerically, the presence of a semicircular groove affects the aerodynamics of the airfoil, resulting in an improved efficiency coefficient of lift, which has risen by 2.25 percent, while the drag coefficient has decreased by 4.32 percent.

Keywords: NACA 0012, Airfoil, Semicircular groove, Angle of attack, Lift and Drag, Separation.

1. Introduction

Aerodynamic efficiency is one of the most important elements impacting the performance of airfoils. In a variety of engineering applications, an airfoil's efficiency may be improved by analyzing the surrounding around it, which is known as the boundary layer, which has a direct influence on the airfoil's dynamic performance. Vortex generators are the most extensively used in the modification process to develop turbulence. The generation of vortices increases the amount of energy in the boundary layer, causing the flow to separate more slowly as a result. A two-dimensional airfoil computational study was carried out and see if the drag might be reduced. It investigates various surface modifications with the goal of reducing overall drag.

Golf balls are a source of inspiration for the concept of extra lift creation. The distance a dimpled golf ball travels is more than that of a smooth ball. Because the dimples on the golf balls create more momentum, they delay flow separation, which lowers the total drag [1].

Rao and Sampath [2] modified the airfoil's surface to improve its performance. A dimple and cylinders were added to a NACA4412 airfoil. Dimples of two sizes were replicated at various locations. Dimples along the trailing edge produced positive results. Distinct sizes of dimples and cylinders were used in five different tests. However, it was discovered that dimples on the airfoil produced a better outcome in terms of airfoil efficiency.

Faruqui et al. [3] The flow control technique was applied in this study. The airfoil utilized was the NACA 4315. The researchers evaluated two alternative models: one with a smooth airfoil and the other with a bumpy surface on the top side of the airfoil. At 80 % of the chord length, the bump was created near the trailing edge. In a smooth airfoil, flow separation begins at around a 9-degree angle of attack. It was discovered that the results of a bumpy-surfaced airfoil changed dramatically as a result.

Mustak and Uddin [4] discussed how to modify the aerodynamic characteristics of an airfoil (NACA-4415) by adding dimples to its surface. The wing model includes dimples on both the outside and inside. A comparison of modified airfoil models with different lift and drag coefficients (AOA). The surface is altered here by taking into account dimples of varying forms. Wake production happens as a result of boundary layer separation when the airfoil achieves a specific angle of attack. For design, Solidworks is utilized. It employs dimples on the surface of the airfoil (NACA-4415) with a consistent cross-section over the span, as well as three wooden airfoil types with and without dimples. Using dimples on the airfoil's top surface slows flow separation, increasing lift force and stall AOA.

Saraf et al. [5] Used CFD software and the k-turbulent model, a two-dimensional airfoil with and without dimples on the upper airfoil NACA0012 surface was investigated. Dimples were measured and compared to smooth airfoils at four different positions. According to our findings, the ideal spot for dimples is at 75 % of the chord length. For various angles of attack, the flow velocity remained constant. The coefficient of lift has been enhanced by 7 %, while the coefficient of drag has been reduced by 3 %.

Yaakub et al. [6] studied the capability of several vortex traps to increase lift at a retreating helicopter blade. Blade Element Theory (BET) and Computational Fluid Dynamics (CFD) calculations are used to determine the effect of the groove on stall delay and to predict flow separation over the airfoil. Three vortex trap structures were analyzed numerically to determine their lift coefficients. The study demonstrated that the presence of a trap increased the lift coefficient and, more crucially, delayed the stall angle.

Domel et al. [7] Improved NACA0012 airfoil aerodynamic performance. Presented a new suction side airfoil designs inspired by denticles. They had varied denticle patterns, diameters, and tilt degrees. Using denticle-inspired surfaces on airfoil may improve lift-to-drag ratio by 323 percent. Streamwise vortices and separation bubbles improve suction.

Al-Jibory and Shinan [8] compared the NACA0012 airfoil with and without a triangular rib using numerical simulations. At 50, 70, and 90 % of the chord length from the leading edge, the triangular rib was utilized as a passive control method on the top surface of the airfoil. The flow was simulated using Workbench Fluent 17.2 software at a fluid velocity of 7 m/s (Re = 78000), attack angles varying from 0 to 22, and a chord length of 168 mm. At low angles of attack (less than 12), the triangular rib on the airfoil's top surface was detrimental to lift and drag results; but, at higher angles, it was beneficial in all locations and outcomes where lift rose and drag decreased. Thus, the performance (lift to drag ratio) of the NACA0012 airfoil was enhanced, although little at 22°. The rib at the 50 % location caused a two-degree delay in the stall angle (from 14 to 16).

The goal of this study is to investigate the effect of a 2 mm diameter semicircular groove on the NACA 0012 airfoil upper surface in several locations to improve the performance of lift and drag at a constant velocity and various angles of attack.

2. Description of Numerical Method

The airfoil NACA 0012 was created with a chord length (152 mm). Structured grids (C-type) were used in airfoil modeling to compare the accuracy of simulation results.

Fig. 1 illustrated the length of the computing domain utilizing a structured grid is 15 times the chord length from the chord line, and the breadth of the computational domain is 20 times the chord length from the leading edig. This allowed for the complete expansion of the airflow. The airfoil surface's first grid line is denoted by the symbol y+ = 1. Fig. 2 illustrates the mesh of the groove.
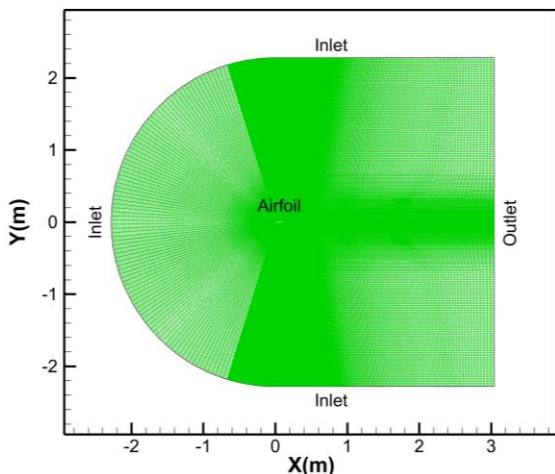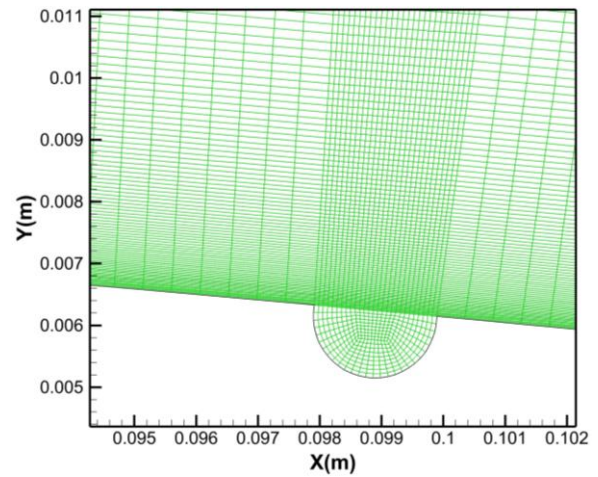

Fig. 1 Structure of Meshing

Fig. 2 Structure of groove mesh.

2.1. Groove Geometry

In this section, the groove geometry is semi-circular with a diameter of (2 mm) with different locations used in the present study. When the airfoil reached its maximum thickness at 30% of the chord, the center of one groove was set at maximum thickness and the airfoil was split into two sections, right and left, each of which was divided into four parts, with the center of the groove placed at the end of the first, second, and third part towards the trailing edge for both left and right sections. It investigates each groove individually, as seen in Table 1.

Table 1. Groove models description.

No.	Groove model	Location in mm from leading edge
1	G1	11.454
2	G2	22.908
3	G3	34.362
4	G4	45.816
5	G5	72.362
6	G6	98.908
7	G7	125.454

2.2. Boundary Condition

The velocity inlet is calculated by two components, x and y, for each angle of attack and in all cases: $x = 20 \cos \alpha$ and $y = 20 \sin \alpha$, where α is the angle of attack in degrees.

Outlet Boundary: The condition of the pressure outlet was set to outflow.

The boundary condition of the airfoil was set to walls.

2.3. Turbulence Model

In order to properly calculate flow near the wall, the shear-stress transport SST-turbulence model use a hybrid approach that combines two models. For boundary layers with unfavorable pressure gradients, it was designed to address the shortcoming of the k-models. Far from the wall, it utilizes a conventional k-model to calculate flow parameters, while a modified k-model uses the turbulence frequency as an additional variable in place of volatile energy (c), which is used in turbulent flow. The k-ω SST two-equation model best matched the published experimental data of other researchers over a broader range of attack angles [9].

3. Results and discussion

3.1. Pressure Contours

Figs. 3-6 shows the pressure contours distribution. The least amount of lift occurs when the angle of attack is 0 degrees. See Fig. 4 and Fig. 5. The stagnation point moved from the leading edge's tip to the lower surface as a result of raising the attack angle, which decreased pressure on the top while increasing pressure on the bottom.
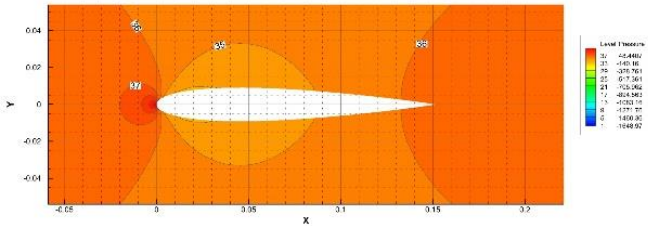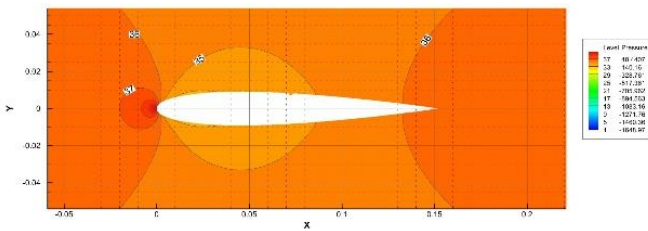
Fig. 3 Smooth airfoil pressure contours at 0°.
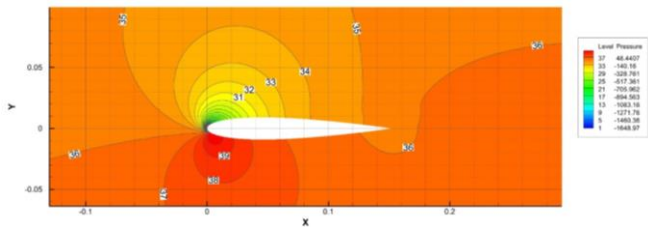
Fig. 4 G6 model airfoil pressure contours at 0°.

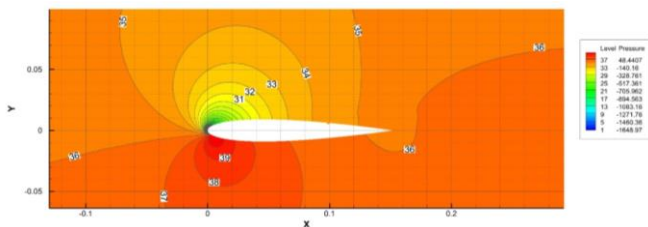**Fig. 5** Smooth airfoil pressure contours at 14°.

Fig. 6 G6 model airfoil pressure contours at 14°.

3.2. Velocity Contours

Figs. 7 and 8 show the velocity contours for a smooth airfoil as well as an airfoil with a groove at an attack angle of 14°. Fig. 7 shows the velocity contours for a smooth airfoil. It should be noted that the flow separation is shown by the darkest regions in the figures, which occur near the leading edge of the airfoil. When comparing the smooth airfoil with the grooved airfoil, it can be plainly observed that the existence of a groove has decreased flow separation, particularly in the G6 model configuration.
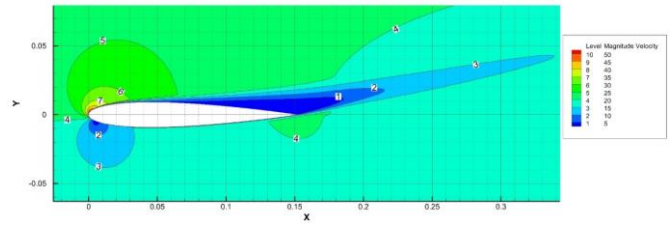
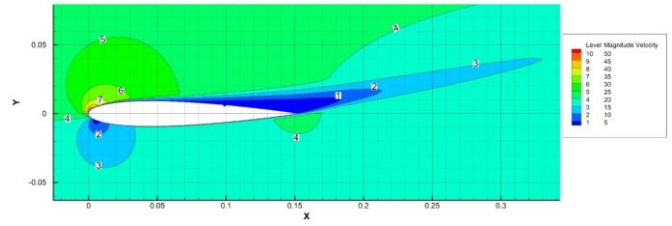**Fig. 7** Smooth airfoil velocity contours at 14°.

Fig. 8 G6 model airfoil velocity contours at 14°.

3.3. Coefficient of Lift and Drag

A CFD study was performed on the 2D NACA0012 model. The coefficient of lift C_l and coefficient of drag C_d for models were calculated using ANSYS Fluent, and the results are shown in Fig. 9 and Fig. 11. It can be shown in Fig. 10 that model G1 produced the poorest results when compared to the smooth airfoil. In the model G6, the coefficient of lift was enhanced while the coefficient of drag was lowered. G2, G3, G4, G5, and G7 grooves were also discovered to be underperforming. To better illustrate the results and compare them to the smooth airfoil, the data were plotted as ΔC_l and ΔC_d, where Δ is the magnitude difference between the modified and smooth airfoils.
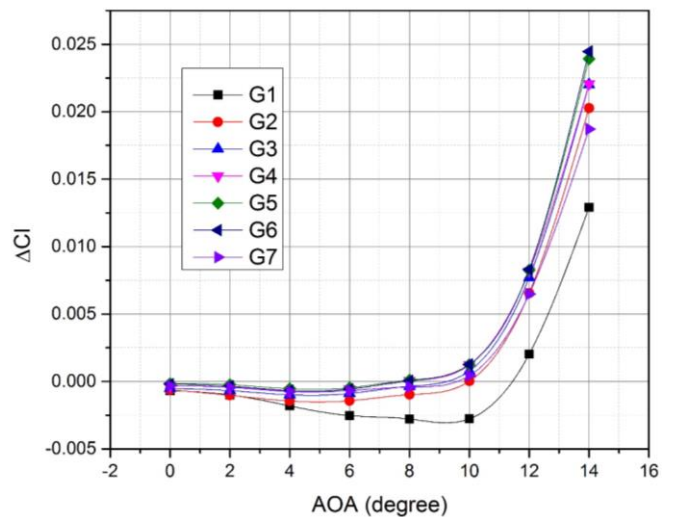
Fig. 9 ΔC_l Vs angles of attack.
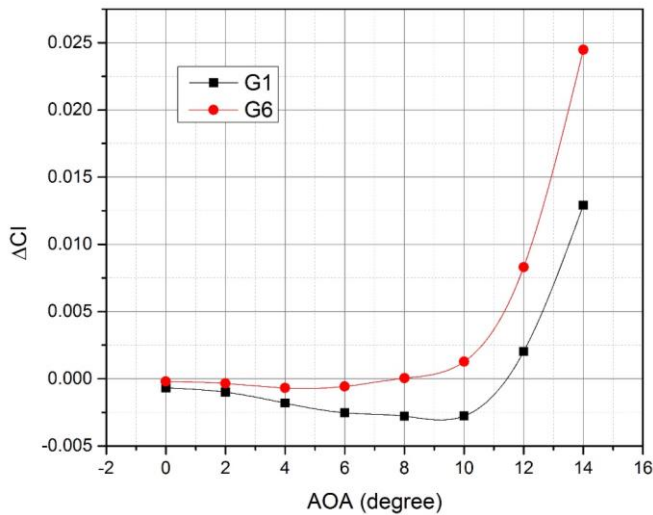
Fig. 10 ΔCl Vs angles of attack.
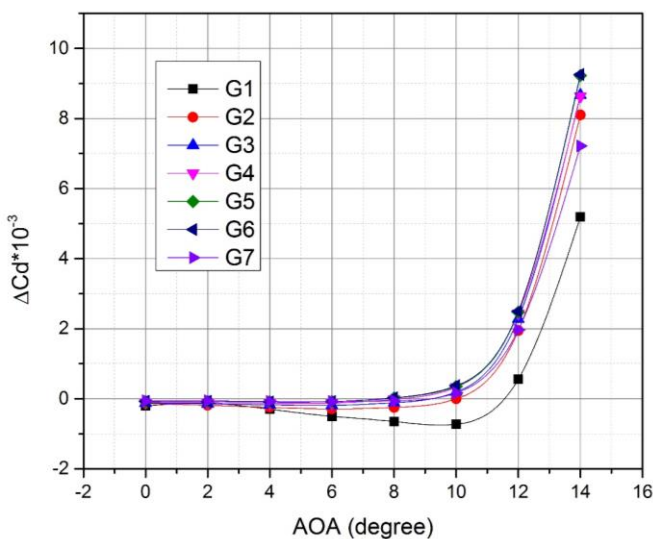

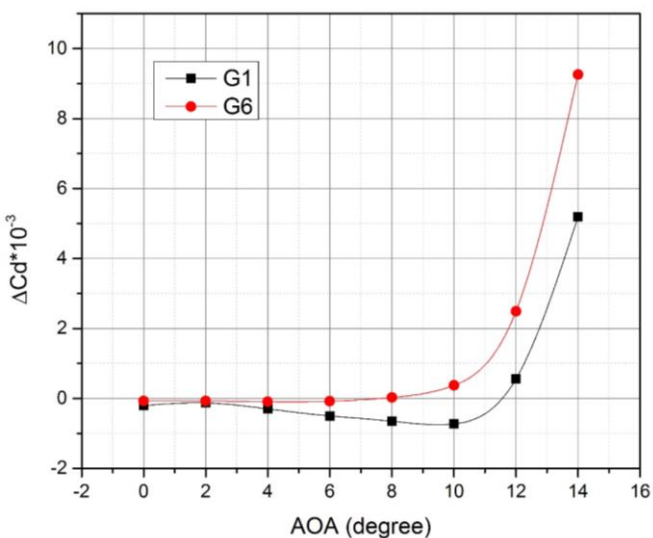**Fig. 11** ΔCd Vs angles of attack.

Fig. 12 ΔCd Vs angles of attack.

4. Conclusions

At a positive angle of attack, the lift and drag coefficients were analyzed and compared to each other. Illustrates that the G6 model's coefficient of lift has risen by 2.25 % when compared with a smooth airfoil. Fig. 11 illustrates the coefficient of drag in the same way. The identical model's drag coefficient was lowered by 4.32 % as well. The position of the groove on the airfoil is crucial. According to our research, the groove on the G6 model is located in the ideal spot.

References

[1] J. M. Davies, "The aerodynamics of golf balls", Journal of Applied Physics, Vol. 20, Issue 9, pp. 821-828, 1949. https://doi.org/10.1063/1.1698540

[2] P. P. Rao, and S. Sampath, "CFD Analysis on Airfoil at High Angles of Attack", International Journal of Engineering Research, Vol. 3, Issue 7, pp. 430-434, 2014. https://www.indianjournals.com/ijor.aspx?target=ijor:ijer&volume=3&issue=7&article=004

[3] S. H. A. Faruqui, M. A. Albari, M. Emran, and A. Ferdaus, "Numerical analysis of role of bumpy surface to control the flow separation of an airfoil", Procedia Engineering, Vol. 90, pp. 255-260, 2014. https://doi.org/10.1016/j.proeng.2014.11.846

[4] R. Mustak, N. Uddin, and M. Mashud "Effect of Different Shaped Dimples on Airfoils", International Conference on Mechanical Engineering and Renewable Energy 2015, November 2015.

[5] A. K. Saraf, M. P. Singh, and T. S. Chouhan, "Effect of Dimple on Aerodynamic Behaviour of Airfoil", International Journal of Engineering and Technology, Vol. 9, No. 3, pp. 2268-2277, 2017. https://doi.org/10.21817/ijet/2017/v9i3/1709030335

[6] M. F. Yaakub, A. A. Wahab, M. F. Abdul Ghafir, S. N. M. M. Yunos, S. J. M. M. Salleh, Q. E. Kamarudin, M. F. M. Masrom, "The aerodynamics investigation of vortex trap on helicopter blade", Applied Mechanics and Materials, Vol. 225, pp. 43-48, 2012. https://doi.org/10.4028/www.scientific.net/AMM.225.43

[7] A. G. Domel, M. Saadat, J. C. Weaver, H. Haj-Hariri, K. Bertoldi, and G. V. Lauder, "Shark skin-inspired designs that improve aerodynamic performance", Journal of the Royal Society Interface, Vol. 15, Issue 139, 2018. https://doi.org/10.1098/rsif.2017.0828

[8] M. W. Al-Jibory and H. A. A. Shinan, "Numerical Study of the Boundary Layer Separation Control on the NACA 0012 Airfoil using Triangular Rib", IOP Conference Series: Materials Science and Engineering, Vol. 671, No. 1, 2020. https://doi.org/10.1088/1757-899X/671/1/012144

[9] G. G. Lee, K. Jang, K. Y. Huh, A. Engineering, and R. Korea, "Evaluation of the Turbulence Models for the Simulation of the Flow Over a National Advisory Committee for Aeronautics (NACA) 0012 Airfoil", Journal of Mechanical Engineering Research, Vol. 4, No. 3, pp. 100-111, 2012. https://doi.org/10.5897/JMER11.074